Journal of Power Sources 219 (2012) 193–198

Contents lists available at SciVerse ScienceDirect

Journal of Power Sources

journal homepage: www.elsevier.com/locate/jpowsour

Reversible and irreversible loss in performance in direct methanol fuel cells during freeze/thaw cycles

Linlin Yang [a,b], Hai Sun [a], Suli Wang [a], Luhua Jiang [a], Gongquan Sun [a,*]

[a] Division of Fuel Cell & Battery, Dalian National Laboratory for Clean Energy, Dalian Institute of Chemical Physics, Chinese Academy of Sciences, Dalian 116023, China
[b] Graduate University of Chinese Academy of Sciences, Beijing 100039, China

HIGHLIGHTS

- ► Investigate the degradation of the DMFC performance during 100 freeze/thaw cycles.
- ► Reversible and irreversible losses in DMFC performance were identified.
- ► A method was put forward to recover the reversible loss in performance.
- ► The voltage @ 100 mA cm^{-2} dropped 16 mV experienced 100 F/T cycles after recovered.

ARTICLE INFO

Article history:
Received 3 June 2012
Received in revised form
6 July 2012
Accepted 7 July 2012
Available online 24 July 2012

Keywords:
Direct methanol fuel cell
Freeze/thaw cycling
Reversible/irreversible performance loss
Reverse current

ABSTRACT

In this paper, the reversible and the irreversible loss in performance of direct methanol fuel cell (DMFC) single cells induced by freeze/thaw cycling are determined and discussed. The reversible loss in performance is attributed to the decreased activity of electrocatalysts due to the strong adsorption of the intermediates from methanol electro-oxidation at subzero temperatures, while the irreversible loss in performance is due to the damage of membrane electrode assembly (MEA) structure. It is found that the reversible degradation of performance is dominant when the cell operated at low current densities with O_2; the irreversible degradation is more obvious when the cell discharged at high current densities or operated with air. A method, applying a reverse current on the single cell, is put forward to recover the reversible loss in performance. By this method, the voltage of the single cell operated with O_2 at 100 mA cm^{-2} drops only about 16 mV after experiencing 100 freeze/thaw cycles between −10 and 60 °C.

1. Introduction

Direct methanol fuel cells (DMFCs) have been attracting much attention as portable power sources because of the high energy density and convenient fuel storage/refilling. One of the challenges for the application of DMFCs are the survivability and cold-start capability in subzero temperatures. Although pure methanol, as the fuel, remains in liquid state in any climatic condition ever measured on the planet [1], typical methanol concentration in use is controlled at a low level (1 M), whose freezing point is −2 °C. DMFCs might suffer from freezing for both anode and the cathode at subzero temperatures, unlike proton exchange membrane fuel cells (PEMFCs), in which water is only produced on the cathode side. The volume expansion of frozen water and frost heave formation would damage the structure of membrane electrode assemblies (MEAs) [2–4]. In addition, the strong adsorption of the intermediates from methanol electro-oxidation at low temperature results in a decrease in catalytic activity [5,6]. Both factors contribute to degradation of the DMFC performance.

Extensive studies on the subzero storage and startup of PEMFCs have been reported [2,4,5,7–17]. The results suggest that the MEA durability against freeze/thaw cycling is able to meet the requirement of automotives [3,4]. However, few studies have been reported on the operation and storage of DMFCs at subzero temperatures [6,18–20]. Presently, the only study reporting the performance and degradation in DMFCs found that MEAs were hard to withstand the freeze/thaw cycling [19].

In this paper, the effects of freeze/thaw cycling on the performance of DMFCs were investigated. We identified two kinds of distinct loss in DMFC performances, one being reversible and related to the decreased activity of catalysts, the other one, being irreversible and related to the damage in MEA structure. Finally, the effects of applying a reverse current on the DMFC performance were investigated by analyzing electrochemical impedance spectroscopy (EIS) of the single cell.

* Corresponding author. Tel./fax: +86 0411 84379063.
E-mail address: gqsun@dicp.ac.cn (G. Sun).

0378-7753/$ – see front matter
http://dx.doi.org/10.1016/j.jpowsour.2012.07.017

2. Experimental

2.1. MEA preparation

The electrodes were prepared using a brush painting method [21]. PtRu/C (Johnson Matthery Inc., Hispec 10000, 60 wt.% PtRu) and Pt/C (Johnson Matthey Inc., Hispec 9100, 60 wt.% Pt) were used as the catalyst for anode and cathode, respectively. The metal loadings for both electrodes were 2.5 mg cm^{-2}. Carbon paper (TGP 060) with a microporous layer was used as gas diffusion layers on both anode and cathode sides. The MEA with an active area of 2 cm × 2 cm were prepared by hot pressing the anode and cathode on either side of a Nafion 115 membrane. Two single cells, Cell I and Cell II, were used in our tests.

2.2. Single cell test procedure

The freeze/thaw cycling test protocol is schematically shown in Fig. 1. It consists of the repetitive steps of cell operation at 60 °C and storage at −10 °C. The cell was cooled down to −10 °C and kept at this temperature for 8 h in an environmental chamber (Giant Force Inc.). In the subsequent heating stage, the cell was taken out of the chamber and heated up to 60 °C by cartridge heaters. Meanwhile the cell was fed with 1 M methanol on a homemade test station.

During the DMFC operation & analysis, the following steps were sequentially operated:

Step 1

1a Constant current mode. The cell discharged at 100 mA cm^{-2} at 60 °C for 30 min. The anode was fed with 1 M methanol aqueous solution at a flow rate of 1 mL min^{-1}; cathode was fed with non-humidified O_2 at a flow rate of 80 mL min^{-1}.

1b i–V curve measurement. The single cell polarizations were obtained using a fuel cell test system (Arbin Instrument Corp.) at 60 °C. A 1 mol L^{-1} methanol aqueous solution was pumped into the anode at a flow rate of 1 mL min^{-1}. Dry oxygen/air was fed to the cathode at a flow rate of 80 mL min^{-1}

Step 2

2a Applying a reverse current. The gas being fed to cathode was switched to nitrogen while keeping anode fed with methanol. Linear sweep voltammetry (LSV) was performed between 0 V and 0.9 V (vs. DHE) at a scan rate of 2 mV s^{-1}. In this case, anode serves as a counter/reference electrode, wherein methanol is oxidized at the cathode, while H_2 is produced in anode side. Gaseous hydrogen formed on the anode removes the adsorbates or reduces the surface oxides.

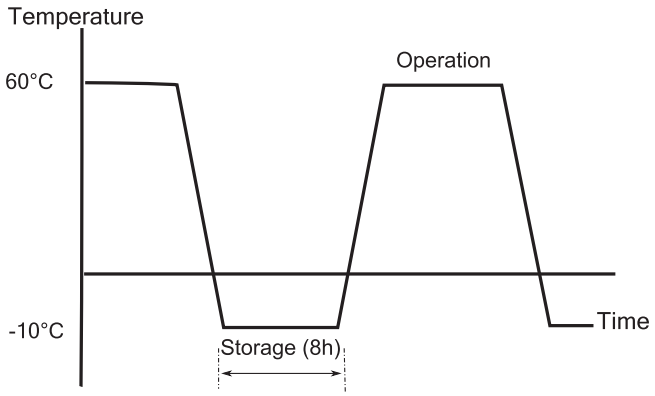

Fig. 1. Schematic of the single cell test procedure with freeze/thaw cycling.

2b i–V curve measurement. see 1b.

2c EIS measurement. EIS measurement was conducted in the frequency range of 1 kHz–100 mHz with 10 steps per decade using a potentiostat (SI 1287, Solartron Analytical) combined with a frequency response analyzer (SI 1260, Solartron Analytical).

2d Anode polarization measurement. The cell was operated in a driven mode using a potentiostat (SI 1287, Solartron Analytical). In this case, hydrogen was fed into the cathode, which served as a counter/reference electrode. The scanned potential range was from 0 to 0.65 V with a sweep rate of 2 mV s^{-1}

2e Cyclic voltammetry (CV) measurement. When the CV of the cathode (or anode) was measured, hydrogen was supplied to the anode (or cathode) to function as a counter/reference electrode, and deionized (DI) water was fed to the cathode (or anode) side at a flow rate of 1 mL min^{-1}. The scanned potential range was from 0 to 1.2 V for cathode or 0–0.65 V for anode with a sweep rate of 20 mV s^{-1}

2f. Feed 1 M methanol solution to anode until a stable single cell polarizations curve was obtained.

Step 1 were performed every cycle, and step 2 were performed every twenty cycles.

2.3. Methanol stripping measurement

The anode (or cathode) was washed by flowing DI water through the electrode chamber for 20 min, then hydrogen was fed to the cathode (or anode) side which served as a counter/reference electrode. The curve was recorded in the potential range between 0 and 0.7 (or 1.2) V with a sweep rate of 20 mV s^{-1}.

3. Results and discussion

3.1. Effects of freeze/thaw cycles

The changes in cell voltage during the 100 freeze/thaw cycles are depicted in Fig. 2. It was found that the cell voltage at a current density of 100 mA cm^{-2} did not change significantly during the 100 freeze/thaw cycles, whereas the fluctuation of the cell voltage

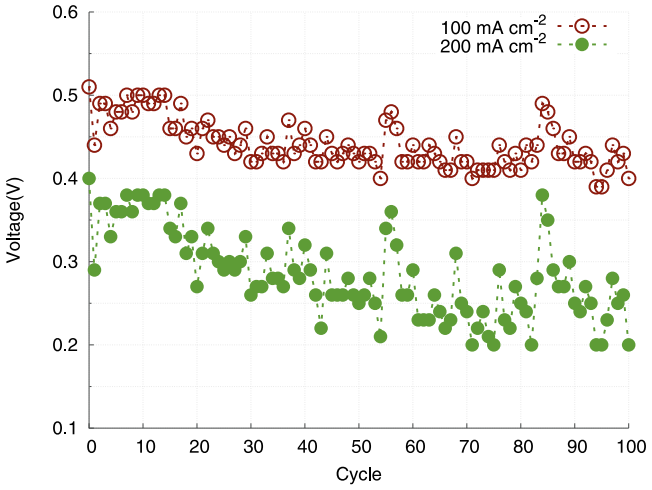

Fig. 2. Voltage change at certain current density during 100 cycle freeze/thaw testing. Cell I, anode: 1 M methanol solution, 1 mL min^{-1}; cathode: nonhumidified O_2, 80 mL min^{-1}.

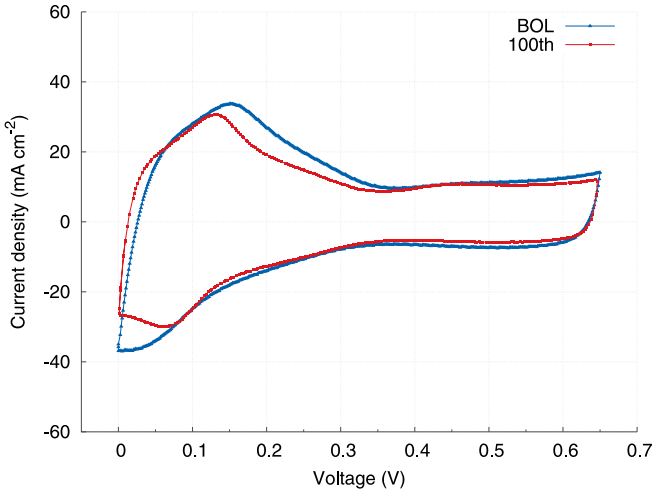

Fig. 3. Cyclic Voltammograms of anode of an MEA before and after freeze/thaw cycles. Cell I, anode: DI water, 1 mL min^{-1}; cathode: H_2, 100 mL min^{-1}.

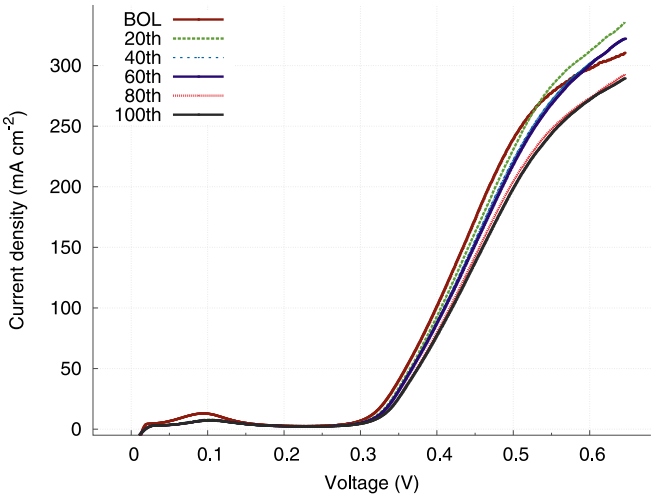

Fig. 5. Anode polarization curves during freeze/thaw cycles. Cell I, anode: 1 M methanol, 1 mL min^{-1}; cathode: nonhumidified H_2, 100 mL min^{-1}.

at a current density of 200 mA cm^{-2} was greater than that of voltage at 100 mA cm^{-2}. The cell performance was improved significantly at the 84th cycle after rested for 26 days, which we would discuss in detail in section 3.2. The fluctuation of the cell voltage at certain current density during freeze/thaw cycles indicates that a reversible degradation might occur during the freeze/thaw cycling.

Cyclic voltammetry was performed to examine the loss in electrochemical surface area (ECSA) after 100 freeze/thaw cycles. ECSA decreased by 19.1% at the anode and by 47.8% at the cathode after 100 free/thaw cycles, as seen in Fig. 3 and Fig. 4. The ECSA losses might result from the structural changes of MEA induced by freezing [4,7,10], and these losses cannot be recovered.

The anode polarization curves are shown in Fig. 5. It can be seen that the overpotential in anode increases with cycling. "Oxygen gain" is referred to the difference in cell voltage between the pair of methanol/O_2 and methanol/air at the same current densities. It is a qualitative indication of mass transfer loss that occurs in an electrode [22]. Fig. 6 is the results of oxygen gain during freeze/thaw cycling, it can be seen that oxygen gains were higher after suffering from subzero temperature than that of beginning of life (BOL). The higher oxygen gains and overpotential in anode after freeze/thaw cycles might result from the damage of MEA structure induced by freezing. Researchers observed the damage of MEA induced by change in volume at phase transformation [3,4,9,10]. This morphological damage of MEAs leads to the performance loss that cannot be recovered, which is referred as the irreversible loss in performance.

3.2. Reversible loss in performance

Fig. 7 shows methanol stripping measurements of a normal MEA and that after subzero temperature storage, it is apparent that the area for methanol oxidation stripping peak became much larger after being stored at low temperatures, indicating that more intermediates from the methanol oxidation reaction (MOR) adsorb on the catalysts for the single cell stored at subzero temperatures. The different behavior of the cells before and after being stored at the subzero temperature in methanol stripping measurements at the same temperature is unexpected and appear to be contrary to thermodynamics; it might be an artifact due to the slow dynamics for the intermediate desorption process which might take a long

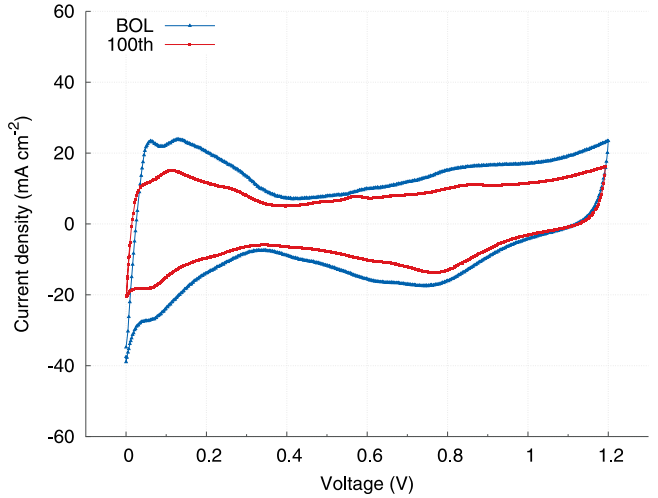

Fig. 4. Cyclic Voltammograms of cathode of an MEA before and after freeze/thaw cycles. Cell I, anode: H_2, 100 mL min^{-1}; cathode: DI water, 1 mL min^{-1}.

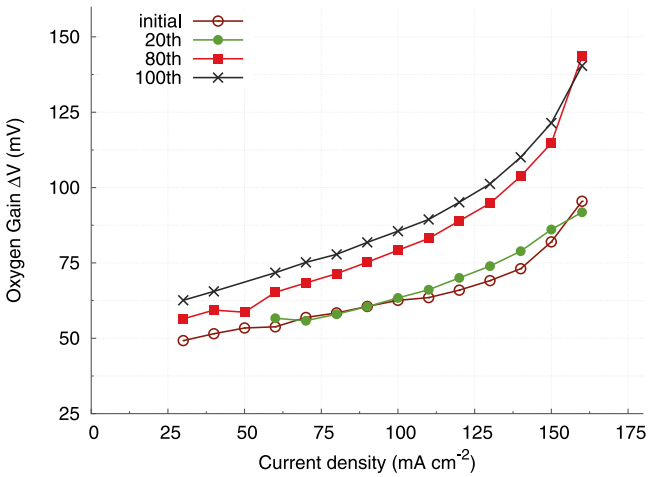

Fig. 6. Oxygen gains of DMFC single cell duing freeze/thaw cycling after recovered. Cell I, anode: 1 M methanol, 1 mL min^{-1}; cathode: nonhumidified O_2/Air, 80 mL min^{-1}.

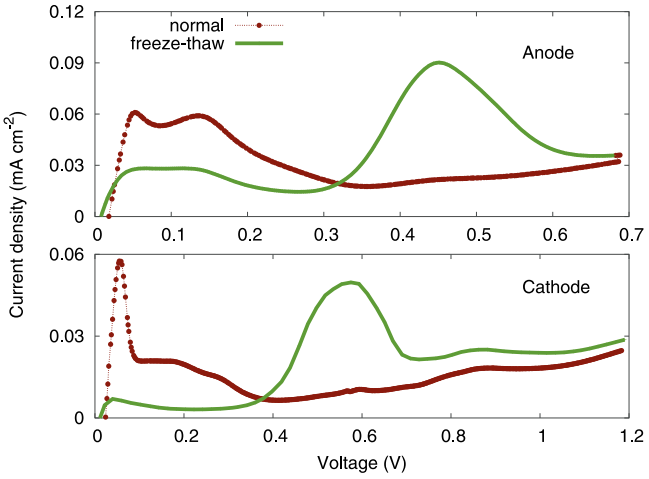

Fig. 7. Methanol stripping measurement of normal MEA and that suffering from freezing. Cell II, 12th freeze/thaw cycle, temperature: 60 °C.

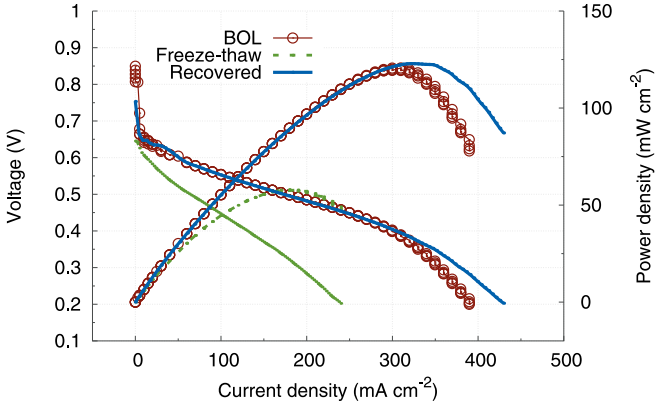

Fig. 8. Typical IV curve before and after applying reverse current. Cell II, 3rd freeze/thaw cycle, anode: 1 M methanol, 1 mL min^{-1}; cathode: nonhumidified O_2, 80 mL min^{-1}.

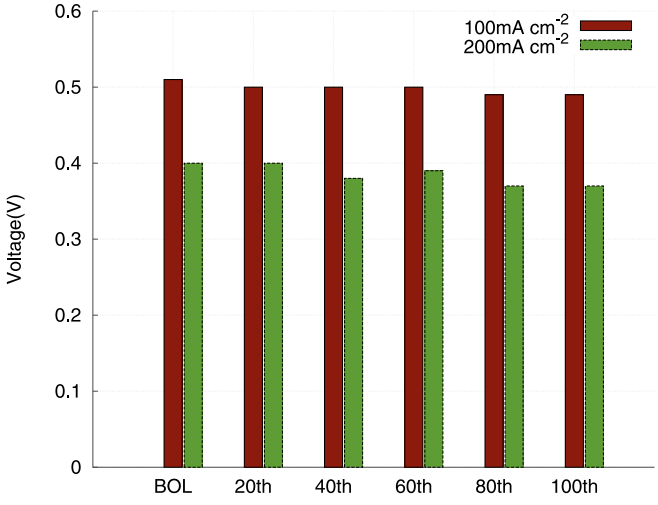

Fig. 9. Voltage change at certain current density during 100 cycle freeze/thaw testing after recovered. Cell I, anode: 1 M methanol, 1 mL min^{-1}; cathode: nonhumidified O_2, 80 mL min^{-1}.

Table 1
Comparion between anode and single cell voltage losses during freeze/thaw cycles at certain current density (cell I).

Potential (mV)	100 mA cm^{-2}			200 mA cm^{-2}		
	BOL	100th	$\|\Delta V\|$	BOL	100th	$\|\Delta V\|$
V_{anode}	398	419	21	468	500	32
$V_{cell,O2}$	506	490	16	400	368	32
$V_{cell,Air}$	446	408	38	380[a]	316[a]	64[a]

[a] At current density of 150 mA cm^{-2}.

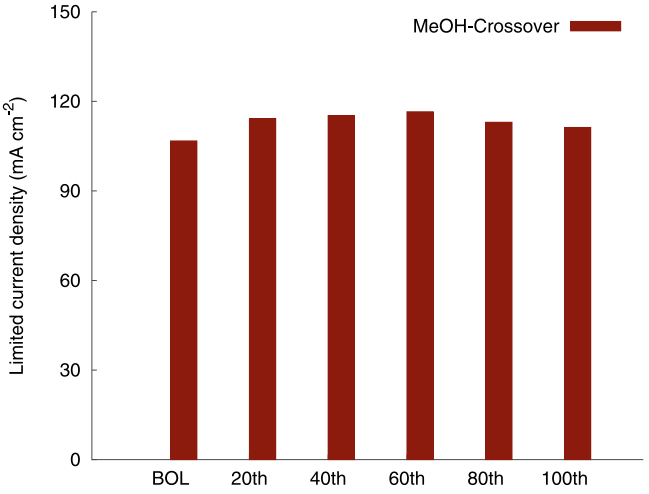

Fig. 10. Methanol crossover limiting current densities during freeze/thaw cycles. Cell I, temperature: 60 °C; anode: 1 M methanol, 1 mL min^{-1}; cathode: N_2, 80 mL min^{-1}.

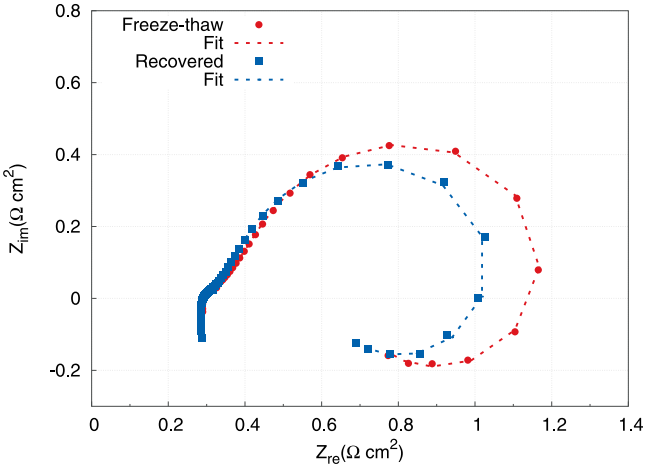

Fig. 11. Experimental and simulated DMFC anode spectra. Cell II, experimental conditions: 60 °C; anode at 0.4 V (vs. DHE), 1 M methanol, 1 mL min^{-1}; cathode: H_2, 100 mL min^{-1}.

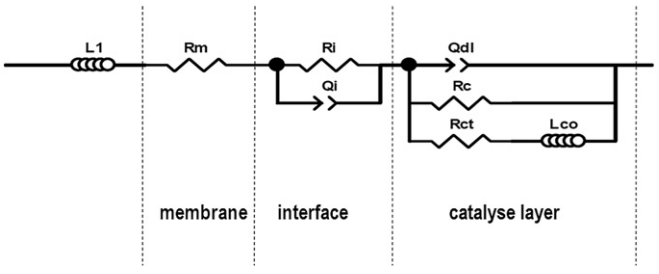

Fig. 12. Equivalent circuit for modeling impedance of DMFC anodes.

Table 2
Fitting parameters for the equivalent circuit model at 0.4 V (vs. DHE).

	R_m (Ω cm^2)	R_i (Ω cm^2)	Q_i (F/cm^2)	n_i	Q_{dl} (F/cm^2)	n_{dl}	R_c (Ω cm^2)	L_{CO} (H/cm^2)	R_{ct} (Ω cm^2)
Freeze-thaw	0.286	0.190	1.059	0.489	0.493	0.958	0.933	0.562	0.306
Recovered	0.282	0.155	1.154	0.505	0.473	1	0.739	0.472	0.279

time to achieve desorption equilibrium after being stored at subzero temperatures. After the 84th freeze/thaw cycle the cell was rested 26 days at room temperature, it is interesting to find that the cell performance is improved significantly, as shown in Fig. 2. This is possibly explained by the less MOR intermediates adsorbed on the catalysts after rest for a long time.

The loss in active area of electrocatalysts leads to the degradation of the cell performance, but this kind of loss can be recovered fully or partially. A method, applying reverse currents to the cell, was put forward to recover the reversible loss in cell performance. This method was previously used for DMFC conditioning [18,23]. As shown in Fig. 8, no performance loss was seen for BOL and that after recovered. Fig. 9 shows the results of voltage at 100 & 200 mA cm^{-2} during freeze/thaw cycling after recovery operation. The performance of the cell, which experienced 100 freeze/thaw cycles, lost slightly after recovered. As mentioned before, the loss in ECSA was found at both electrodes. However, no valid correlation between the loss in ECSA and performance loss is built up to now [4]. The slight degradation after 100 freeze/thaw cycles might be attributed to: (1) the high catalyst loading (compare to PEMFCs) making the cell performance less sensitive to the loss in ECSA; (2) sufficiently open space in the catalyst layer (CL) with a porous structure allowing the swelling in volume that avoid a damage to the CL structure [3,24]; (3) the depression of the freezing point for water (aqueous methanol) in the MEA leads to partial water existing in liquid state [4,25,26].

The loss in performance of the DMFC operated with air was larger than that operated with O_2 (see Fig. 6), indicating an increase in mass-transport resistance in cathode. For a DMFC operated with O_2, convection is the main way for oxygen transport across the GDL, while for the one operated with air, diffusion is the dominant way for oxygen transport [27]. As a consequence, the overall performance of the cell fed with air is more sensitive to the changes in pore structures resulting from freeze damage than that fed with O_2.

Table 1 summarizes the measured cell voltage and anode potential based on the experimental data shown in Figs. 5, 6 and 9. It can be seen that the loss in anodic voltage contributes to the overall losses in the cell voltage for the DMFC operated with oxygen. However, it is not the case for a cell operated with air, indicating that freeze/thaw cycles lead to an increase in mass-transport resistance. In summary, both electrodes suffer degradation during freeze/thaw cycles.

3.3. *Effects of applying a reverse current to the single cell on its performance*

Fig. 10 summarizes the limiting currents from methanol crossover during 100 freeze/thaw cycling. A considerable amount of fuel crossover from anode to cathode owing to the permeability of methanol through the perfluorosulfonic acid membranes, which might be one of the most frequently heard disadvantages of DMFCs. However, tailoring to the methanol crossover, we put forward a reverse current method by which an electrical current of polarity opposite to that in a working DMFC was passed through the MEA to recover the cell performance [23]. When applying a reverse current, a positive voltage was applied to the cathode, and oxidized the crossovered methanol at the cathode, gaseous hydrogen is formed on the anode which can removes the adsorbates. By doing this, the reversible loss in performance can be recovered.

Electrochemical impedance spectroscopy is a powerful tool for electrical characterization. It can provide information about the change in process occurring in the electrode before and after applying a reverse current. We examine the effects of reverse current on the anode side, because oxidation of the crossovered methanol also take place during normal operation at the cathode. Fig. 11 is the Nyquist plots of the DMFC anode before and after recovered. The impedance model for the anode employed in this study is shown in Fig. 12. R_m denotes the resistance of the membrane and R_i represents the resistance of the interface between the membrane and the catalyst layer; R_{ct} denotes the charge transfer resistance; Q_{dl} is the double layer capacitance; R_c represents the resistance of the solid phase in catalyst layer; L_{CO} is the inductance due to the slowness of the relaxation of $(CO)_{ads}$ coverage [28,29]. It can be seen that the simulated spectrum using model shown in Fig. 12 agrees well with the experimentally observed plots. From the analyses of the fitting parameters listed in Table 2, it was found that L_{CO}, an indicator of the amount of $(CO)_{ads}$ on the catalyst surfaces, decreased 19% after recovered, suggesting $(CO)_{ads}$ is removed after applying a reverse current.

4. Conclusion

The present study shows that the loss in performance of the DMFCs due to the freeze/thaw (−10 °C/60 °C) cycling includes both the reversible and the irreversible degradation of cell performance. The reversible degradation is attributed to the decreased activity of catalyst due to the strong adsorption of MOR intermediates where the performance loss can be recovered by applying a reverse current, while irreversible degradation is related to structural changes of MEA. Reversible loss in performance is dominant over the irreversible loss, and only slight irreversible degradation of performance of the cell operated with O_2 is observed after 100 freeze/thaw cycles. However, noticeable irreversible degradation is found when the cell operated at high current density or fed with air because of the larger mass-transport resistance.

The approach applying a reverse current is confirmed a valid method to recover the reversible loss in performance by removing the strong intermediates from the MOR on the catalyst surface. After applying a reverse current, the cell voltage at 100 mA cm^{-2} only dropped 16 mV (from 506 mV to 490 mV) over the course of the 100 freeze/thaw cycles.

Acknowledgments

This work was supported by the National 863 High-Tech Project (2009AA05Z121).

References

[1] F. Zenith, U. Krewer, Energy and Environmental Science. 4 (2011) 519–527.
[2] J.P. Meyers, Subfreezing Phenomena in Polymer Electrolyte Fuel Cells, in: Polymer Electrolyte Fuel Cell Durability, Springer Verlag, 2009.
[3] C.Y. Wang, X.G. Yang, Y. Tabuchi, F. Kagami, Cold-start Durability of Membrane-electrode Assemblies, in: Handbook of Fuel Cells, John Wiley & Sons, Ltd, 2010.

[4] A.-K. Srouji, M.M. Mench, Freeze Damage to Polymer Electrolyte Fuel Cells, in: Polymer Electrolyte Fuel Cell Degradation, Academic Press, 2011.
[5] J. St-Pierre, J. Roberts, K. Colbow, S. Campbell, A. Nelson, Journal of New Materials for Electrochemical Systems 8 (3) (2005) 163–176.
[6] J.-Y. Park, S.-J. Song, J.-H. Lee, J.-H. Kim, H. Cho, International Journal of Hydrogen Energy 35 (15) (2010) 7982–7990.
[7] M. Oszcipok, D. Riemann, U. Kronenwett, M. Kreideweis, M. Zedda, Journal of Power Sources 145 (2) (2005) 407–415.
[8] M. Oszcipok, M. Zedda, J. Hesselmann, M. Huppmann, M. Wodrich, M. Junghardt, C. Hebling, Journal of Power Sources 157 (2) (2006) 666–673.
[9] Q. Guo, Z. Qi, Journal of Power Sources 160 (2) (2006) 1269–1274.
[10] S. Ge, C.-Y. Wang, Journal of the Electrochemical Society 154 (12) (2007) B1399–B1406.
[11] S. Ge, C.-Y. Wang, Electrochimica Acta 52 (14) (2007) 4825–4835.
[12] J. Hou, B. Yi, H. Yu, L. Hao, W. Song, Y. Fu, Z. Shao, International Journal of Hydrogen Energy 32 (17) (2007) 4503–4509.
[13] E.L. Thompson, J. Jorne, H.A. Gasteiger, Journal of the Electrochemical Society 154 (8) (2007) B783–B792.
[14] E.L. Thompson, J. Jorne, W. Gu, H.A. Gasteiger, Journal of the Electrochemical Society 155 (6) (2008) B625–B634.
[15] E.L. Thompson, J. Jorne, W. Gu, H.A. Gasteiger, Journal of the Electrochemical Society 155 (9) (2008) B887–B896.
[16] K. Jiao, X. Li, International Journal of Hydrogen Energy 34 (19) (2009) 8171–8184.
[17] W. Song, H. Yu, L. Hao, B. Yi, Z. Shao, International Journal of Hydrogen Energy 35 (20) (2010) 11129–11137.
[18] U. Krewer, J. Park, J. Lee, H. Cho, C. Pak, D. You, Y. Lee, Journal of Power Sources 187 (1) (2009) 103–111.
[19] H.-C. Cha, C.-Y. Chen, R.-X. Wang, C.-L. Chang, Journal of Power Sources 196 (5) (2011) 2650–2660.
[20] Y.-C. Park, D.-H. Peck, S.-K. Kim, S. Lim, D.-H. Jung, D.-Y. Lee, International Journal of Hydrogen Energy 36 (9) (2011) 5655–5665.
[21] Q. Mao, G. Sun, S. Wang, H. Sun, G. Wang, Y. Gao, A. Ye, Y. Tian, Q. Xin, Electrochimica Acta 52 (24) (2007) 6763–6770.
[22] S.S. Kocha, Principles of Mea Preparation, in: Handbook of Fuel Cells, John Wiley & Sons, Ltd, 2010.
[23] C. Rice, X. Ren, S. Gottesfeld, Methods of conditioning direct methanol fuel cell, US Patent, 6,962,760 (2003).
[24] X.G. Yang, Y. Tabuchi, F. Kagami, C.-Y. Wang, Journal of the Electrochemical Society 155 (7) (2008) B752–B761.
[25] M. Sliwinska-Bartkowiak, G. Dudziak, R. Sikorski, R. Gras, K.E. Gubbins, R. Radhakrishnan, Phys. Chem. Chem. Phys. 3 (2001) 1179–1184.
[26] C. Alba-Simionesco, B. Coasne, G. Dosseh, G. Dudziak, K.E. Gubbins, R. Radhakrishnan, M. Sliwinska-Bartkowiak, Journal of Physics: Condensed Matter 18 (6) (2006) 15–68.
[27] J. Benziger, E. Kimball, R. Mejia-Ariza, I. Kevrekidis, AIChE Journal 57 (9) (2011) 2505–2517.
[28] N. Hsu, S. Yen, K. Jeng, C. Chien, Journal of Power Sources 161 (1) (2006) 232–239.
[29] J.T. Müller, P.M. Urban, W.F. Hölderich, Journal of Power Sources 84 (2) (1999) 157–160.